MAGNETOHYDRODYNAMIC FLOW AND HEAT TRANSFER OF NON-NEWTONIAN POWER-LAW NANOFLUID OVER A ROTATING DISK WITH HALL CURRENT

by

Abdel-Aziz SALEM[a,b*] and Rania FATHY[c]

[a] Department of Mathematics, Faculty of Science and Arts, Qassim University, Al-Muznib, Saudi Arabia
[b] Department of Mathematics, Faculty of Science, Suez Canal University, Ismailia, Egypt
[c] Department of Mathematics, Faculty of Science, Zagazig University, Sharkia, Egypt

Original scientific paper
https://doi.org/10.2298/TSCI151009123S

This work studies the flow and heat transfer of a power-law nanofluid in the presence of an axial uniform magnetic field in the vicinity of a constantly rotating infinite disk. The Hall current effect is taken into consideration. The governing momentum and energy equations are solved numerically by the shooting method. Some of the results obtained for a special case of the problem are compared to the results published in a work of Abo-Eldahab [37] and are found to be in excellent agreement. The effects of the solid fraction,the magnetic interaction number, the Hall current, and the viscosity index, on the velocity and temperature profiles as well as the local skin friction coefficients and the heat transfer rate are shown graphically.

Key words: *nanofluid, rotating disk, heat transfer, Hall current*

Introduction

Rotating disk flow has been at the center of a large number of theoretical and experimental studies in recent years. This is mainly due to its many applications in engineering, such as rotating machinery, lubrication, oceanography, computer storage devices, viscometers, and crystal growth processes. The rotating disk problem was first solved by Von Karmam [1]. He showed that the Navier-Stokes equations for steady flow of a Newtonian incompressible fluid due to a disk rotating far from other solid surface can be reduced to a set of ODE. These equations can be solved by using an approximate integral method. Cochran [2] obtained asymptotic solutions for the steady hydrodynamic problem formulated by Von Karman. Benton [3] improved the steady-state solutions given by Cochran and extended the problem to transient state.

The rotating disk and stability issues were attacked theoretically, numerically and experimentally by many authors amongst many others, such as Hall [4], and Jarrae and Chauve [5]. The influence of an external uniform magnetic field on the flow due to a rotating disk was studied by Attia and Hassan [6]. Also, the effect of uniform suction or injection through a rotating porous disk on the steady hydrodynamic flow has been investigated by some researchers [7-10]. The effect of thermal radiation on the steady laminar convective hy-

* Corresponding author, e-mail: azizsalem32@hotmail.com

drodynamic flow of a viscous and electrically conducting fluid due to a rotating disk has considered by Devi and Devi [11]. The study of hydromagnetic flows with the Hall current has important engineering applications in problems of MHD generators and Hall accelerations as well as in flight MHD. Hassan and Attia [12] investigated the steady MHD boundary-layer flow due to an infinite disk rotating with uniform angular velocity in the essence of an axial magnetic field. They neglected induced magnetic field but considered the Hall current and accordingly solved steady-state equation numerically using a finite difference approximation. The effect of Hall current on steady laminar convective hydrodynamic flow of an electrically conducting fluid over a porous rotating infinite disk has been examined by Devi and Devi [13]. Recently, Khidir [14] investigated the effects of viscous dissipation and ohmic heating on steady MHD convective flow due to a porous rotating disk with variable properties. A number of studies have been reported in the literature focusing on nanofluids because of their industrial and engineering applications, such as electronics, transportation as well as nuclear reactors and biomedicine. Nanofluids can be also used in various biomedical applications like cancer therapeutics, nanodrug delivery, nanocryosurgery, and cryopreservation. Choi [15] was the first to introduce the term nanofluid to represent a fluid in which nanoscale particles (nanoparticles) are suspended in a base fluid with a low thermal conductivity such as water, ethylene glycol and oils [16, 17]. The concept of nanofluids, in recent years, has been proposed as a route for surpassing the performance of heat transfer rate in regular fluids. Experimental studies show that even with a small volumetric fraction of nanoparticles (usually less than 5%), the thermal conductivity of the base fluid is enhanced by 10-50% with a remarkable improvement in the convective heat transfer coefficient, see [18-23]. Bachok *et al.* [24] investigated the steady flow of an incompressible viscous fluid due to a porous rotating disk in a nanofluid via the Keller-box method. They considered two models for the effective thermal conductivity of the nanofluid. They also reported different behaviors for the heat transfer rate at the surface for these methods. Recently, the flow and heat transfer characteristic over a rotating disk immersed in five distinct nanofluids have been investigated by Mustafa [25].

One type of non-Newtonian fluid is the power-law fluid. These fluids are characterized by the property that during its motion the stress is a non-linear function of the rate of strain. Many of the inelastic non-Newtonian fluids encountered in chemical engineering processes, are known to follow the empirical Ostwald-de Waele model or the so-called *power-law model*. In this model the shear stress varies according to a power function of the strain rate. Acrivos *et al*. [26] investigate the flow of a non-Newtonian fluid (power-law fluid) on a rotating disk. Numerical solution for the flow caused by a disk rotating in liquids with a shear dependent viscosity was first obtained by Mistschka and Ulbricht [27]. Wichterle and Mitschka [28] revised the same study, with a focus on a shear of liquid particles to fit the application of micro-mixing technology. Andersson *et al*. [29] reconsidered the problem of Mistschka and Ulbricht [27] to test the reliability of their numerical solutions when considering shear-thickening fluids beyond those considered by Mitschka and Ulbricht. The influence of an external magnetic field on the flow due to a rotating disk was studied by several authors [30-32]. Some interesting effects of magnetic field on the flow of a power-law fluid over a rotating disk was examined by Andersson and Korte [33]. In all these investigations, the effects of the Hall current were not considered. Recently, the effects of Hall currents on hydromagnetic flow due to a rotating disk have been studied by Hassan and Attia [34], Attia and Hassan [35] and Abdul Maleque and Abdus Sttar [36]. Abo-Eldahab and Salem [37] considered the MHD flow and heat transfer of non-Newtonian power-law fluid with diffusion and chemical reac-

tion on a moving cylinder. Chunying *et al.* [38] studied the steady flow and heat transfer of a viscous incompressible power-law fluid over a rotating disk.

The aim of the present work is to study the flow and heat transfer due to a rotating disk immersed in a power-law nanofluid in the presence of Hall current using a nanofluid model proposed by Tiwari and Das [39]. The system of non-linear PDE is transformed into coupled non-linear ODE by means of Von Karman similarity variables and solved numerically by Rung-Kutta method coupled with Shooting technique [40]. The radial, tangential, axial velocities, and temperature profiles are sketched for different values of solid volume fraction parameter, power-law index, magnetic field and Hall parameter. The effects of these parameters are discussed.

Formulation of the problem

We consider a steady, laminar, axi-symmetric flow of an incompressible non-Newtonian nanofluid driven solely by an infinite rotating disk. As shown in fig. 1. Let (r, φ, z) be the set of cylindrical co-ordinates and let the disk rotate with constant angular velocity Ω and be placed at $z = 0$. The surface of the disk is maintained at a uniform temperature T_w, while the temperature of the free stream is T_∞. An external strong magnetic field is applied in the positive z-direction and has flux density B_o.

The generalized Ohm's law including Hall current is given in the form [41]:

$$\vec{J} = \sigma\left[\vec{E} + \vec{V} \times \vec{B} - \frac{1}{en_e}(\vec{J} \times \vec{B})\right] \qquad (1)$$

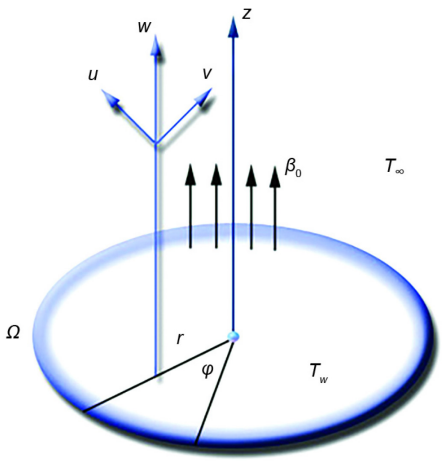

Figure 1. Physical model and co-ordinate system

where $\vec{V} = u\vec{e}_r + v\vec{e}_w + w\vec{e}_z$ is the velocity vector, $\vec{B} = (0, 0, B_o)$ – the magnetic induction vector, $\vec{E}$ – the electric field vector, $\vec{J}$ – the current density vector, $\sigma = (e^2 n_e t_e / m_e)$ – the electrical conductivity, t_e – the electron collision time, e – the electron charge, n_e – the electron number density, and m_e – the mass of the electron. In the low-magnetic Reynolds number approximation, the induced magnetic field can be ignored. Since no applied or polarization voltage is imposed on the flow field, the electric field vector $\vec{E}$ is equal to zero**.** For large values of the magnetic field strength, the generalized Ohm's law, given by eq. (1), in the absence of an electric field can be solved for $\vec{J}$ to yield:

$$J_r = \frac{\sigma B_0}{1+m^2}(mv - u), \quad J_\varphi = \frac{\sigma B_0}{1+m^2}(v + mu) \qquad (2)$$

where $m = w_e t_e$ is the Hall parameter with $w = eB_0/m_e$ as the electron frequency. It is assumed that the base fluid and the nanoparticles are in thermal equilibrium and no slip occurs between them. The thermophysical properties of the fluid and nanoparticles are given in tab. 1. [22].

Under these assumptions with the usual boundary-layer approximation and using the nanofluid model proposed by Tiwari and Das [39], the governing equations for the conserva-

tion of mass, momentum and energy for the problem under consideration (in the presence of Hall current) can be written:

$$\frac{\partial u}{\partial r}+\frac{u}{r}+\frac{\partial w}{\partial r}=0 \tag{3}$$

$$u\frac{\partial u}{\partial r}-\frac{v^2}{r}+w\frac{\partial u}{\partial z}=-\frac{1}{\rho_{\mathrm{nf}}}\frac{\partial p}{\partial r}+\frac{1}{\rho_{\mathrm{nf}}}\frac{\partial}{\partial z}\cdot$$

Table 1. Thermophysical properties of the base fluid and the nanoparticles

Physical properties	Fluid phase (water)	Cu
c_p [Jkg^{-1}K^{-1}]	4179	385
ρ [kgm^{-3}]	997.1	8933
k [Wm^{-1}K^{-1}]	0.613	400
$\alpha\cdot10^7$ [m^{2}s^{-1}]	1.47	1163.1

$$\cdot\left\{\mu_{\mathrm{nf}}\left[\left(\frac{\partial u}{\partial z}\right)^2+\left(\frac{\partial v}{\partial z}\right)^2\right]^{\frac{n-1}{2}}\frac{\partial u}{\partial z}\right\}-\frac{\sigma B_0^2}{\rho_{\mathrm{nf}}(1+m^2)}(u-mv) \tag{4}$$

$$u\frac{\partial v}{\partial r}+\frac{uv}{r}+w\frac{\partial v}{\partial z}=\frac{1}{\rho_{\mathrm{nf}}}\frac{\partial}{\partial z}\left\{\mu_{\mathrm{nf}}\left[\left(\frac{\partial u}{\partial z}\right)^2+\left(\frac{\partial v}{\partial z}\right)^2\right]^{\frac{n-1}{2}}\frac{\partial v}{\partial z}\right\}-\frac{\sigma B_0^2}{\rho_{\mathrm{nf}}(1+m^2)}(v+mu) \tag{5}$$

$$u\frac{\partial T}{\partial r}+w\frac{\partial T}{\partial z}=\frac{1}{\rho_{\mathrm{nf}}}\frac{\partial}{\partial z}\left\{k_{\mathrm{nf}}\left[\left(\frac{\partial u}{\partial z}\right)^2+\left(\frac{\partial v}{\partial z}\right)^2\right]^{\frac{n-1}{2}}\frac{\partial T}{\partial z}\right\} \tag{6}$$

$$-\frac{\partial p}{\partial z}=0 \tag{7}$$

The boundary conditions are:

$$u=w=0,\quad v=\Omega r,\quad T=T_{\mathrm{w}}\qquad \text{at}\quad z=0\quad \text{and}\quad u=v=0,\quad T=T_{\infty}\qquad \text{as}\quad z\to\infty \tag{8}$$

where u, v and w are velocity components in the directions of increasing r, ϕ, z, respectively.

$$\mu=\mu_{\mathrm{nf}}\left[\left(\frac{\partial u}{\partial z}\right)^2+\left(\frac{\partial v}{\partial z}\right)^2\right]^{\frac{n-1}{2}}$$

is the effective viscosity of nanoliquid, μ_{nf} – the modified consistency viscosity coefficient, ρ_{nf} – the effective density of nanoliquid, and n – the flow behavior index. The fluid is Newtonian for $n = 1$. The fluid is termed pseudplastic (or shear thinning) for $n < 1$ and dilatant (or shear thickening) for $n > 1$. Following Zheng *et al.* [42] we assume the thermal conductivity is power-law dependent on velocity:

$$k=k_{\mathrm{nf}}\left[\left(\frac{\partial u}{\partial z}\right)^2+\left(\frac{\partial v}{\partial z}\right)^2\right]^{\frac{n-1}{2}}$$

where k is the effective thermal conductivity of nanoliquid, and k_{nf} is the modified thermal conductivity of the nanoliquid. The properties of nanofluids are defined [17]:

$$\rho_{\mathrm{nf}} = (1-\varphi)\rho_{\mathrm{f}} + \varphi\rho_{\mathrm{s}}, \quad \mu_{\mathrm{nf}} = \frac{\mu_{\mathrm{f}}}{(1-\varphi)^{2.5}}, \quad \alpha_{\mathrm{nf}} = \frac{k_{\mathrm{nf}}}{(\rho c_p)_{\mathrm{nf}}}$$

$$(\rho c_p)_{\mathrm{nf}} = (1-\varphi)(\rho c_p)_{\mathrm{f}} + \varphi(\rho c_p)_{\mathrm{s}}, \quad \frac{k_{\mathrm{nf}}}{k_{\mathrm{f}}} = \frac{(k_{\mathrm{s}}+2k_{\mathrm{f}}) - 2\varphi(k_{\mathrm{f}}-k_{\mathrm{s}})}{(k_{\mathrm{s}}+2k_{\mathrm{f}}) + 2\varphi(k_{\mathrm{f}}-k_{\mathrm{s}})} \tag{9}$$

where ϕ is the solid volume fraction of nanoliquid, μ_{f} – the viscosity of the basic fluid, ρ_{s} – the density of the solid, $(\rho c_p)_{\mathrm{f}}$ – the heat capacity of the base fluid, $(\rho c_p)_{\mathrm{s}}$ – the heat capacity of solid, k_{f} thermal conductivity of base fluid, and k_{s} thermal conductivity of solid. By introducing the Von Karaman transformation [1], one finds that:

$$u = r\Omega F(\eta), \quad v = r\Omega G(\eta), \quad w = \left(\frac{\Omega^{1-2n}}{\frac{k}{\rho}}\right)^{-\frac{1}{n+1}} r^{\frac{n-1}{n+1}} H(\eta), \quad \theta(\eta) = \frac{T-T_\infty}{T_{\mathrm{w}}-T_\infty} \tag{10}$$

where

$$\eta = z\left(\frac{\Omega^{2-n}}{\frac{k}{\rho}}\right)^{-\frac{1}{n+1}} r^{\frac{1-n}{1+n}} \tag{11}$$

is the generalized dimensionless similarity variable originally proposed by Mitschka [43], and F, G, and H are non-dimensional functions of η.

In the present study the magnetic interaction number, M, was investigated to be $M = \sigma B_o^2/\rho\Omega$ which represents the ratio between the magnetic force to the fluid inertia force. With these definitions, eqs. (3)-(6), eq. (8) takes the form:

$$H' + 2F + F'\frac{1-n}{1+n}\eta = 0 \tag{12}$$

$$\frac{1}{(1-\phi)^{2.5}\left(1-\phi+\phi\frac{\rho_{\mathrm{s}}}{\rho_{\mathrm{f}}}\right)}\frac{\mathrm{d}}{\mathrm{d}\eta}\left[(F'^2+G'^2)^{\frac{n-1}{2}}F'\right] - \left(H+\frac{1-n}{1+n}F\eta\right)F' - F^2 + G^2 -$$

$$-\frac{M}{1+m^2}(F-mG) = 0 \tag{13}$$

$$\frac{1}{(1-\phi)^{2.5}\left(1-\phi+\phi\frac{\rho_{\mathrm{s}}}{\rho_{\mathrm{f}}}\right)}\frac{\mathrm{d}}{\mathrm{d}\eta}\left[(F'^2+G'^2)^{\frac{n-1}{2}}G'\right] - \left(H+\frac{1-n}{1+n}F\eta\right)G' - 2FG -$$

$$-\frac{M}{1+m^2}(mF+G) = 0 \tag{14}$$

$$\frac{1}{\mathrm{Pr}}\frac{\dfrac{k_{\mathrm{nf}}}{k_{\mathrm{f}}}}{1-\phi+\phi\dfrac{(\rho c_p)_{\mathrm{s}}}{(\rho c_p)_{\mathrm{f}}}}\frac{\mathrm{d}}{\mathrm{d}\eta}\left[(F'^2+G'^2)^{\frac{n-1}{2}}\theta'\right]-\left(H+\frac{1-n}{1+n}F\eta\right)\theta'=0 \tag{15}$$

where the prime denote the differentiation with respect to similarity variable η. Boundary conditions are:

$$F=0,\quad G=1,\quad H=0,\quad \theta=1\quad \text{at}\quad \eta=0\ \text{and}\ F=0,\quad G=0,\quad \theta=0\quad \text{as}\quad \eta\to\infty \tag{16}$$

Results and discussion

The system of transformed eqs. (12)-(15) with the corresponding boundary conditions (16) have been solved numerically by means of the fourth-order Runge-Kutta method with systematic estimates of $F'(0)$, $C'(0)$, and $\theta'(0)$ by shooting technique. In the present calculations, step size of $\Delta\eta = 0.001$ and $\eta_{\max} = 15$ were found to be satisfactory in obtaining sufficient accuracy within a tolerance less than 10^{-8} in nearly all cases. Comparison is made with the available published data in tab. 2 for $F'(0)$, $G'(0)$, and $-H(\infty)$ which show a good agreement with the present results.

Table 2. Comparison of some of the present data with results of Anderson and Korte [33] for the particular case of a Newtonian fluid (n = 1) and for m = 0

M	$F'(0)$		$G'(0)$		$-H(\infty)$	
	[33]	Present	[33]	Present	[33]	Present
0	0.5101	0.51023254	0.6160	0.61592206	0.8827	0.88447335
0.5	0.3851	0.38513252	0.8487	0.84872382	0.4589	0.45888794
1	0.3093	0.30925791	1.0691	1.06905343	0.2533	0.25331375
2	0.2306	0.23055903	1.4421	1.44209404	0.1086	0.10858343
4	0.1657	0.16570305	2.0103	2.01026675	0.0408	0.04077522

The effects of solid volume fraction, ϕ, on the velocity profiles in the radial, tangential, and axial directions, F, G, and $-H$ for a shear-thinning fluid ($n < 1$) and a shear-thickening fluid ($n > 1$) are shown in figs. 2(a)-2(c). Due to the existence of the centrifugal force, the radial velocity attains a maximum value close to the surface of the disk for all values of ϕ. With increasing the values of solid volume fraction parameter, radial velocity increases near the surface of the disk, but towards the end it decreases. Also, the rate of its convergence to its limiting value (*i. e.* zero) is faster for larger value of ϕ and n. In figs. 2(a) and 2(b), we observe that, far from the surface of the disk, the radial and tangential velocity profiles decreases as n increases. The reason for such behavior is that increasing the power-law index n tends to increase the viscous forces and decelerate the flow, thus decreasing the velocity profiles. Moreover, for n = 1.5, the axial flow, fig. 2(c) fails to approach an asymptotic limit for large η in a regular manner as two other velocity components, F and G, tend to zero at the edge of the boundary-layer. This observation can easily be ascribed to an anticipated deterioration of the numerical accuracy caused by the thickening of the boundary-layer.

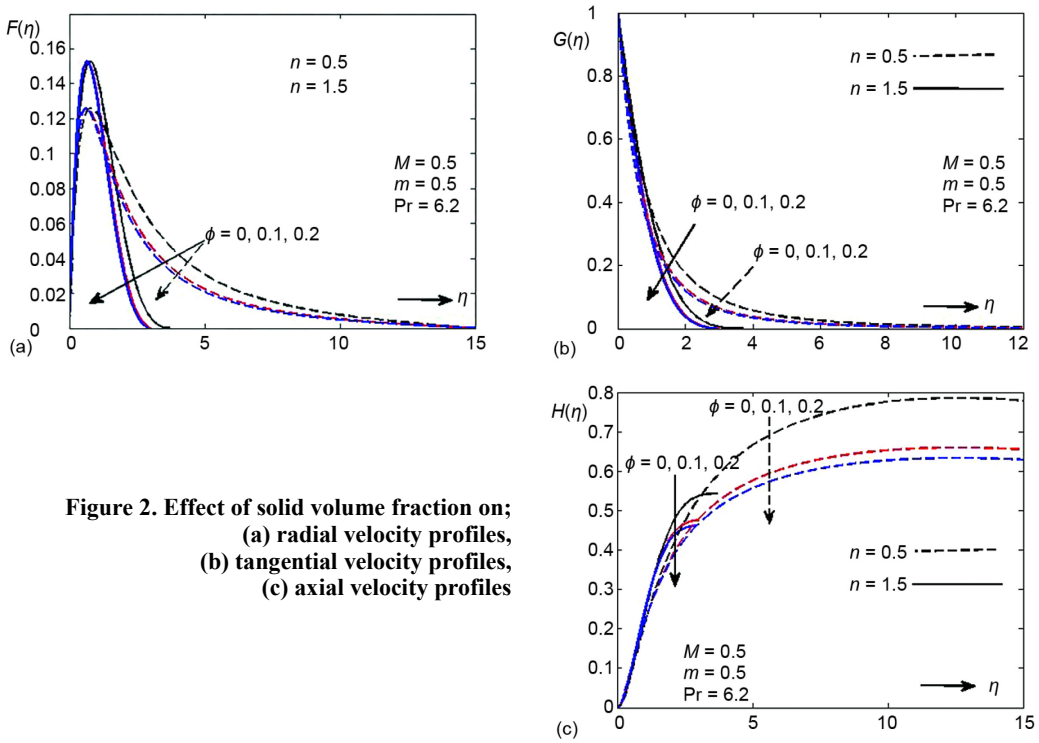

Figure 2. Effect of solid volume fraction on; (a) radial velocity profiles, (b) tangential velocity profiles, (c) axial velocity profiles

Figure 3 shows the influence of solid volume fraction, ϕ, on the temperature distributions for two different values of the power-law index n. The dimensionless temperature profiles $\theta(\eta)$ decrease monotonically from T_m (*i. e.* $\theta = 1$)at the surface of the disk to T_∞ (*i. e.* $\theta = 0$) at infinity. With increase in the solid volume fraction, ϕ, the temperature increases across the boundary-layer for both values of the power-law index $n <$ 1 and $n >$ 1. Also, the temperature distribution across the boundary-layer slightly increases with increase in values of n due to the little enhancement of the viscous forces, but the effect is opposite far away from the surface of the disk.

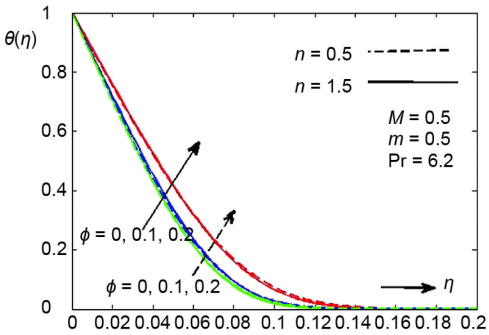

Figure 3. Effect of solid volume fraction on the temperature profiles

Figures 4(a)-4(c) depicts the variation of velocity profiles in the radial, tangential, and axial distributions, *F, G*, and *–H* for different values of n and M. Application of a magnetic field produces a resistive force called the Lorentz force. This force has a tendency to slow the flow around the disk. This is depicted by the decreases in the radial, tangential, and axial velocity profiles as M increases, as shown in figs. 4(a)-4(c). The magnetic field effect is also observed to be more pronounced at lower values of M and n because a nanofluid with a thinning boundary--layer is more susceptible to magnetic force effects. Also, for a large value of n (= 1.5), the axial flow, fig. 4(c) fails to approach an asymptotic limit for large η in a regular manner as two other velocity components, F and G, tends to zero at the edge of the boundary-layer.

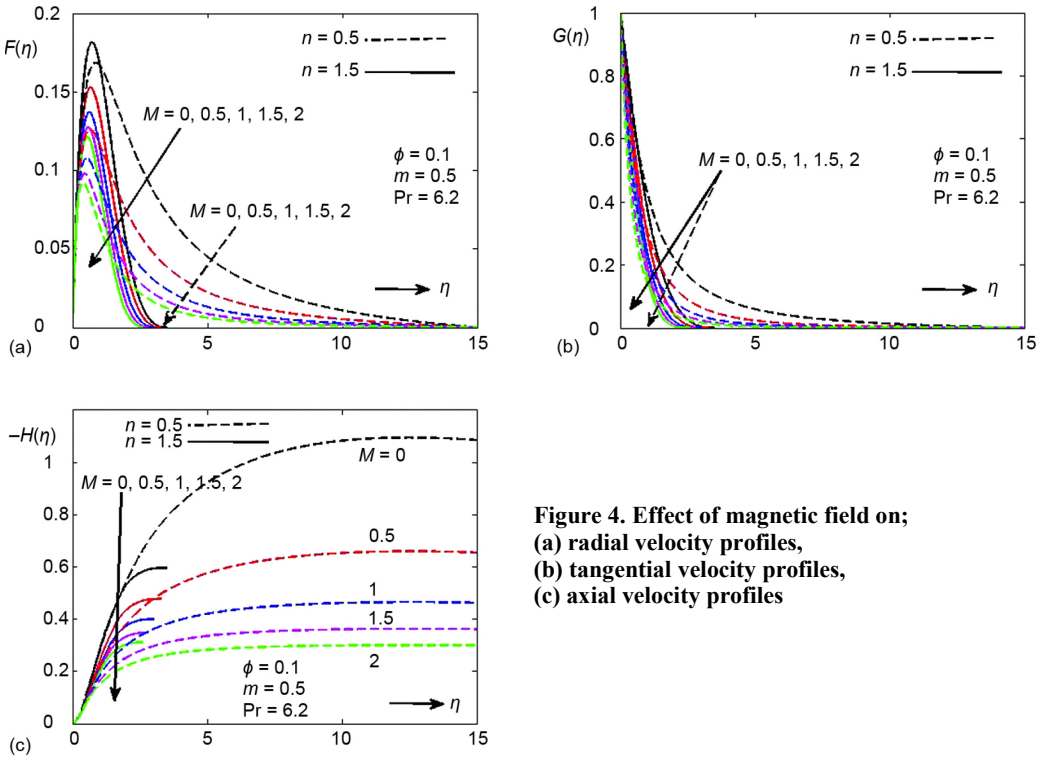

Figure 4. Effect of magnetic field on;
(a) radial velocity profiles,
(b) tangential velocity profiles,
(c) axial velocity profiles

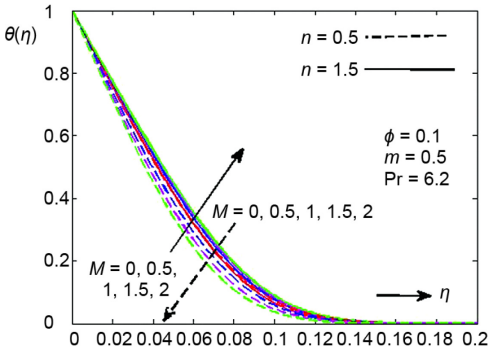

Figure 5. Effect of magnetic field on the temperature profiles

Figure 5 reveals the influence of magnetic field, M, on the temperature profile for pseudo-plastic and dilatants nanofluids. The temperature profile may be enhanced or reduced by increasing M, depending on the fluid index, n. In this figure it is observed that the temperature decreases with increasing M for pseudo-plastic nanofluid ($n < 1$), but increases with M for dilatant nanofluid ($n > 1$). Also, the influence of M is more obvious for a pseudo-plastic nanofluid than for a dilatants nanofluid.

Figures 6(a)-6(c) show the radial, tangential, axial velocities, and temperature at different values of the Hall current, m, for pseudo-plastic nanofluid. The radial and axial velocity profiles increase due to the increase in the magnitude of m in the interval $0 \leq m \leq 5$, see figs. 6(a) and 6(c). However, beyond $m = 5$, the radial and axial velocity profiles decrease as the Hall parameter m increases. Furthermore, this decrease in F and $-H$ is almost negligible for large m ($m > 60$). The phenomenon for small and large values of the Hall parameter m has been explained by Hassan and Attia [34]. The tangential velocity profiles G, as shown in fig. 6(b), are found to increase for all values of Hall parameter, m. Figure 7 shows that the temperature profile decreases for $m \leq 1.5$, and increases for $m > 1.5$. This increase in θ is almost negligible for large values of m.

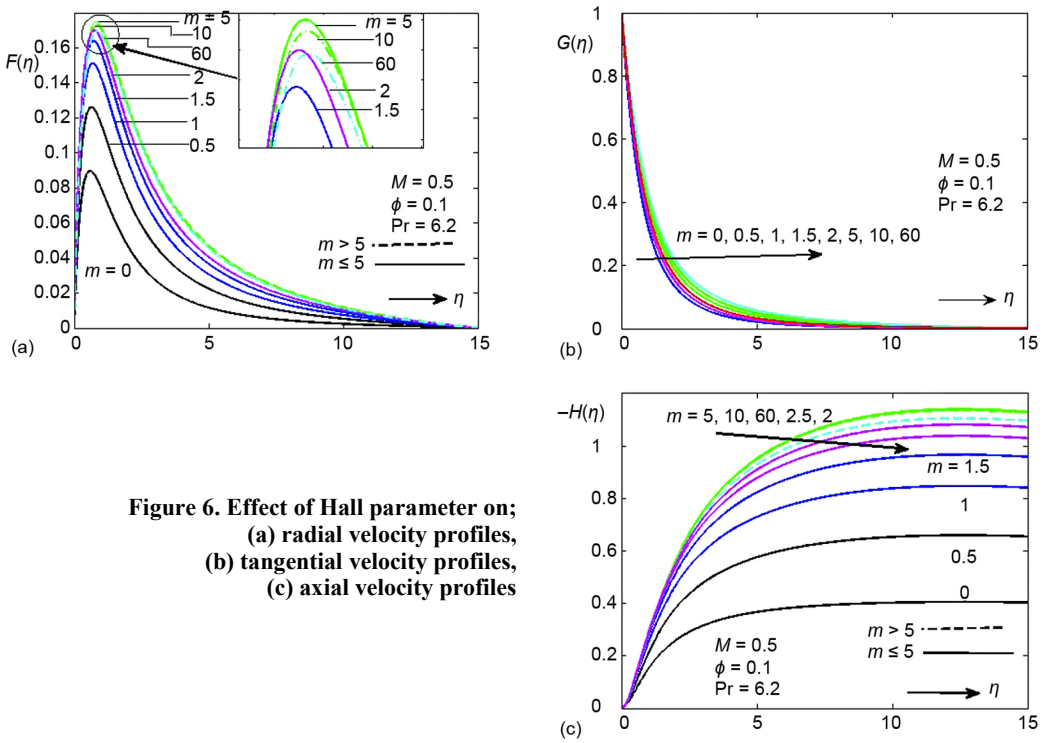

Figure 6. Effect of Hall parameter on; (a) radial velocity profiles, (b) tangential velocity profiles, (c) axial velocity profiles

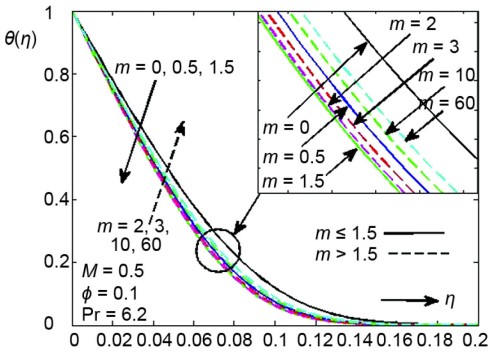

Figure 7. Effect of Hall parameter on the temperature profiles

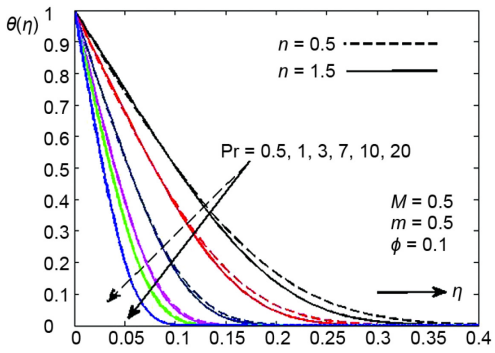

Figure 8. Effect of Prandtl number on the temperature profiles

Figure 8 shows the usual effect of Prandtl number, on the temperature profiles for pseudo-plastic and dilatants nanofluids. It can be seen that Prandtl number decreases the temperature distribution throughout the boundary-layer. This is due to the fact that there would be a decrease of thermal boundary-layer thickness with the increase of Prandtl number. In addition, the temperature profile is less affected by the fluid index n for Pr = 20. This behavior implies that the fluid of smaller Prandtl number is more responsive to fluid index n than the fluid having a larger Prandtl number.

Finally, the values of the radial and tangential skin frictions $F'(0)$ and $G'(0)$ at the disk surface, as well as the axial inflow $-H(\infty)$ and heat flux on the surface $-\theta'(0)$ are plotted against the power-law index n in figs. 9 and 10. We observe that an increase in the value of

the solid volume fraction parameter ϕ may lead to a decrease in the radial skin friction, $F'(0)$, and the axial inflow, $-H(\infty)$, yet it increases the tangential skin friction coefficient, $G'(0)$, and rate of heat transfer, $-\theta'(0)$. It is also to note that the radial skin friction decreases with n for various values of the solid volume fraction, ϕ. However the trend is reversed for large ϕ, especially when the fluid is dilatant nanofluid ($n > 1$).

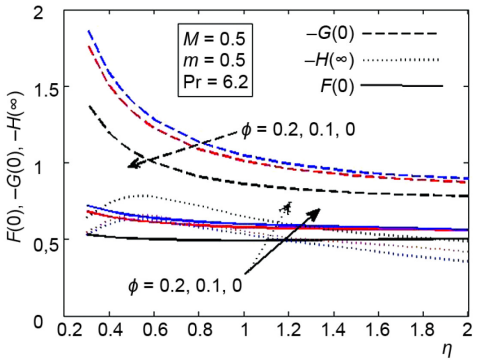

Figure 9. Effect of solid volume fraction on $F'(0)$, $-G'(0)$, $-H(0)$

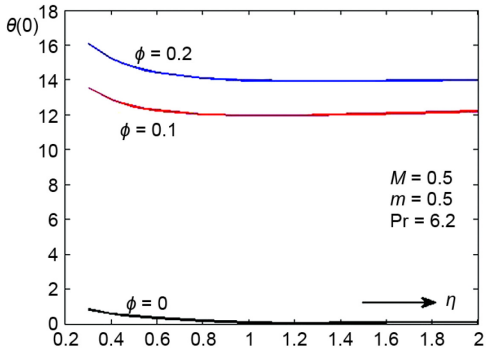

Figure 10. Effect of solid volume fraction on the rate of heat transfer $-\theta'(0)$

Conclusions

The present work deals with the MHD flow and heat transfer of non-Newtonian power-law nanofluid due to a rotating disk. The governing fundamental equations are approximated by a system of non-linear ODE by using a similarity transformation, and are solved numerically by using the Rung-Kutta and shooting methods. The numerical results obtained agree very well with the previously published data in some particular cases of the present study. The effects of the solid volume fraction, ϕ, and the magnetic interaction number, M, on nanofluid velocity and temperature are discussed for shear-thinning and shear-thickening non-Newtonian nanofluis. The highlights of this study are as follows.

- The solid volume fraction decreases the magnitude of the axial and tangential nanofluid velocity components and increases the magnitude of the radial nanofluid velocity component and temperature profiles throughout the boundary-layer.
- The obtained numerical results show that the Hall parameter, m, has an interesting effect on the radial and axial nanofluid velocity profiles. For large values of $m > 5$, the resistive effects of the magnetic field are diminished, hence, the radial and axial nanofluid velocity profiles decrease with the increase of m while the tangential nanofluid velocity profile increases for all values of m.
- The temperature profile decreases with increasing m in the range $0 \leq m \leq 1.5$, while for $m > 1.5$, the temperature profile increases with increasing m.
- The magnetic field has increasing effects on the temperature profiles for dilatant non-Newtonian nanofluid, whereas the opposite is observed for pseudo-plastic non-Newtonian nanofluid.

Nomenclature

$\vec{B}$ – external uniform magnetic field, [kgs^{-2}A^{-1}]
B_o – constant magnetic flux density, [kgs^{-2}A^{-1}]
c_p – specific heat at constant pressure, [Jkg^{-1}K^{-1}]
$\vec{E}$ – electric field vector
e – charge of electron
$\vec{J}$ – current density

k – thermal conductivity
m – Hall parameter
n_e – number density of electrons
(r, φ, z) – cylindrical polar co-ordinates
T – fluid temperature, [K]
t_e – electron collision time
u – radial velocity
v – tangential velocity
w – axial velocity

Greek symbols

η – a scale boundary-layer coordinate
θ – self-similar temperature
μ – dynamic viscosity, [Nsm^{-2}]
ρ – density, [kgm^{-3}]
σ – electrical conductivity(s/m)
ϕ – nanoparticale volume fraction

Subscripts

e – number density of electrons
f – fluid phase
s – solid phase
w – condition of the wall
∞ – ambient condition

References

[1] Von Karman, T., Über Laminare und Turbulente Reibung, *ZAMM1, 4* (1921), pp. 233-235
[2] Cochran, W. G., The Flow due to a Rotating Disk, *Proceedings, Cambridge Phileos. Soc., 30,* (1934), 3, pp. 365-375
[3] Benton, E. R., On the Flow due to a Rotating Disk, *J. Fluid Mech., 24* (1966), 4, pp. 781-800
[4] Hall, P., An Asymptotic Investigation of the Stationary Modes of Instability of the Boundary Layer on a Rotating Disk, *Proc Roy. Soc. London Ser. A, 406* (1986), 1830, pp. 93-106
[5] Jarre, S. L. G., Chauve, M. P., Experimental Study of Rotating Disk Instability, *Phys. Fluids*, *8* (1996), 2, pp. 496-508
[6] Attia, H. A., Hassan, A., On Hydromagnetic Flow Due to a Rotating Disk, *Appl. Math. Model, 28* (2004), 12, pp. 1007-1014
[7] Kelson, N., *et al*., Note on Porous Rotating Disk, *ANZIAM J., 42* (2000), pp. 837-855
[8] Maleque, Kh. A., *et al*., The Effect of Variable Properties on Steady Laminar Convective Flow due to a Porous Rotating Disk, *ASME J. Heat Transfer*, *127* (2005), 12, pp. 1406-1409
[9] Sparrow, E. M., *et al*.., Mass Transfer Flow and Heat Transfer About a Rotating Disk, *ASME J. Heat Transfer*, *82* (1960), 4, pp. 294-302
[10] Turkyilmazoglu, M., Exact Solution for the Incompressible Viscous Fluid of Porous Rotating Disk, *Int. Non-linear Mech*., *44* (2009), 4, pp. 352-357
[11] Devi, S. P., Devi, R., On Hydromagnetic Flow due to Rotating Disk with Radiation Effects, *Nonlinear Analysis:Modeling Control*, *16* (2011), 1, pp. 17-29
[12] Hassan, A. L., Attia, H. A., Flow due to Rotating Disk with Hall Effect, *Phys. Letter A, 228* (1997), 4-5, pp. 246-290
[13] Devi, S. P., Devi, R., Effects of Thermal Radiation on Hydromagnetic Flow due to a Porous Rotating Disk with Hall Effect, *J. of Applied Fluid Mechanics, 5* (2012), 2, pp. 1-7
[14] Khidir, A. A., Viscous Dissipation, Ohmic Heating and Radiation effects on MHD Flow Past a Rotating Disk Embedded in a Pporous Medium with Variable Properties, *Arab. J. Math*., *2* (2013), 3, pp. 263-277
[15] Choi, S. U. S., Enhancing Thermal Conductivity of Fluids with Nanoparticles, *Proceedings*, ASME International Mechanical Engineering Congress and Exposition, San Francesco, Cal., USA, ASME, FED 231/MD, 1995, pp. 99-105
[16] Wang, X. Q., Mujumdar, A. S., Heat Transfer Characteristics of NanoFluids: a Review*, Int. J. Ther. Sci*., *46* (2007), 1, pp. 1-19
[17] Khanafer, R., *et al*., Buoyancy-Driven Heat Transfer Enhancement in a Two-Dimensional Enclosure Utilizing Nanofluids*, Int. J. Heat Mass Transfer, 46* (2003), 19, pp. 3639-3653
[18] Masuda, H., *et al*., Altering the Thermal Conductivity and Viscosity of Liquid by Dispersing Ultra-Fine Particles, *Netsu Bussei, 4* (1993), 7, pp. 227-233
[19] Das, S., Temperature Dependence of Thermal Conductivity Enhancement for Nanofluids*, J. Heat Transfer*, *125* (2003), 4, pp. 567-574)
[20] Pak, B. C., Cho, Y., Hydrodynamic and Heat Transfer Study of Dispersed Fluids with Submicron Metallic Oxide Particles, *Exp. Heat transfer*, *11* (1998), 2, pp. 151-170
[21] Xuan, Y., Li, Q., Investigation on Convective Heat Transfer and Flow Features of Nanofluids, *J. Heat Transfer*, *125* (2003), 1, pp. 151-155

[22] Eastman, J. A., *et al*., Anomalously Increased Effective Thermal Conductivity of Ethylene Glycol-Based Nanofluids Containing Copper Nano Particles*, Appl. Phys. Lett*., *78* (2001), 6, pp. 718-725
[23] Minsta, H. A., *et al*., New Temperature Dependent Thermal Conductivity Data for Water-Based Nanofluids, *Int. j. Therm. Sci., 48* (2009), 2, pp. 363-371
[24] Bachok, N., *et al*., Flow and Heat Transfer over a Rotating Porous Disk in a Nanofluid, *Physica A*, *406* (2011), 9, pp. 1767-1772
[25] Mustafa, T., Nanofluid Flow and Heat Transfer due to a Rotating Disk, *Computers &Fluids*, *94* (2014), May, pp. 139-146
[26] Acrivos, A., *et al*., On the Flow of a Non-Newtonian Liquid on a Rotating Disk, *J. of Applied Physics, 31* (1960), 6, pp. 963-968
[27] Mitschka, P., Ulbricht, J., Nicht-Newtonsche Flüssigkeiten IV. Strömung Nicht-Newtonscher Flüssigkeiten Ostwald-de-Waeleschen Ttyps in der Umgebung Rotierender Drehkegel und Scheiben, NCollect. *Czech. Chem. Commun. 30* (1965), 8, pp. 2511-2526
[28] Wichterle, K., Mitschka, P., Relative Shear Deformation of Non-Newtonian Liquids in Impeller Induced Flow, *Collect. Czech. Chem. Commun*., *63* (1998), 12, pp. 2092-2102
[29] Andersson, H. I., *et al*., Flow of a Power-Law Fluid over a Rotating Disk Revisited*, Fluid Dynamics Research*, *28* (2001), 2, pp. 75-88
[30] El-Mistikawy T. M. A., Attia, H. A., The Rotating Disk Fflow in the Presence of Strong Magnetic Field, *Proceedings*, 3rd Int. Cong. of Fluid Mech., Cairo, Egypt, Vol. 3, 1990, pp. 1211
[31] Hossian, Md. A., *et al.*, Unsteady Flow of Viscous Incompressible Fluid with Temperature-Dependent Viscosity due to a Rotating Disk in Presence of Transverse Magnetic Field and Heat Transfer, *Int. J. Therm. Sci.*, *40* (2001), 1, pp. 11-20
[32] Takhar, H. S., *et al*., Unsteady MHD Flow and Heat Transfer on a Rotating Disk in Ambient Fluid, *Int. J. Therm. Sci., 41* (2002), 2, pp. 147-155
[33] Andersson H. I., Korte, E. De., MHD Flow of a Power-Law Fluid Over a Rotating Disk, European J. of Mechanics B/Fluids, *21* (2002), 3, pp. 317-324
[34] Hassan A. L. A., Attia, H. A., Flow due to a Rotating Disk with Hall Effect, *Phys. Lett. A*., *228* (1997), 4-5, pp. 246-290
[35] Attia, H. A. Hassan, A. A. L., On Hydromagnetic Flow due to a Rotating Disk, *Applied Mathematical Modelling*, *28* (2004), 12, pp. 1007-1014
[36] Abdul Maleque, Kh., Abdus, Sttar, Md., The Effects of Variable Properties and Hall Current on Steady MHD Laminar Cconvective Fluid Flow Due to a Porous Rotating Disk, *Int. J. of Heat and Mass Transfer*, *48* (2005), 23-24, pp. 4963-4972
[37] Abo-Eldahab, E. M., Salem, A. M., MHD Flow and Heat Transfer of Non-Newtonian Power-Law Fluid with Diffusion and Chemical Reaction on Moving Cylinder, *Heat Mass Transfer*, *41* (2005), 8, pp. 703-708
[38] Chunying, M., *et al*., Steady Flow and Heat Transfer of the Power-Law Fluid over a Rrotating Disk, *Int. Comm. In Heat and Mass Transfer, 38* (2011), 3, pp. 280-284
[39] Tiwari, I. K. Das, M. K., Heat Transfer Augmentation in a Two-Sided Lid-Driven Differentially Heated Square Cavity Utilizing Nanofluids, *Int. J. Heat Mass Trans.*, *50* (2007), 9-10, pp. 2002-2018
[40] Zwillinger, D., *Handbook of Differential Equations,* 2nd ed., Academic Press, New York, USA, 1992
[41] Stton, G. W., Sherman, A., *Engineering Magnetohydrodynamics*, McGraw-Hill, New York*,* USA, 1965
[42] Zheng, H., *et al*., Fully Developed Convective Heat Transfer of Power Law Fluids in Circular Tube, *Chinese Physics Letters*, *25* (2008), 1, pp. 195-197
[43] Mitschka, P., Nicht-Newtonische Flüssigkeiten II. Drehströmung Ostwald-de Waelescher Nicht-Newtonischer Flüssigkeiten. *Coll. Czech. Chem. Comm*., *29* (1964), 12, pp. 2892-2905

Paper submitted: October 9, 2015
Paper revised: March 19, 2016
Paper accepted: March 24, 2016